

Polymorphism of phenethylammonium bromide: the effect of particle properties on the thermodynamics

M.J.M. Van Oort¹ and M.L. Cotton*

Merck Frosst Centre for Therapeutic Research, P.O. Box 1005, Pointe Claire-Dorval, PQ H9R 4P8 (Canada)

(Received 31 August 1992)

Abstract

The solid–solid phase transition in phenethylammonium bromide $C_6H_5CH_2CH_2NH_3Br$ was investigated using differential scanning calorimetry (DSC), IR spectroscopy, powder X-ray diffraction and hot-stage microscopy. The volume change associated with the phase transition caused the crystals to shatter. Single crystals gave a single extremely sharp endotherm in the DSC thermal curves obtained but different crystals gave significantly different transition temperatures over at least 5°C range (≈ 61 to $\approx 66^\circ C$). Multiple crystals gave multiple peaks within the same DSC experiment even when cleaved from the same single crystal. Polycrystalline samples produced DSC thermal curves which were much broader and the transition temperature appeared to increase with a decrease in particle size. On average, small crystals ($\approx 38 \mu m$) had a transition temperature ($76^\circ C$) about $13^\circ C$ higher than large crystals ($\approx 63^\circ C$). The enthalpy of transition of the small crystals was about $500 J mol^{-1}$ lower and the entropy of transition was $0.3 R$ lower than the large crystals. These investigations suggest that the thermodynamic properties vary with the particle properties which are dependent on particle size and particle size changes occurring with thermal cycling.

INTRODUCTION

Thermally-induced polymorphism in ammonium salts and substituted ammonium salts has been the subject of many experimental and theoretical studies [1]. Differential scanning calorimetric (DSC) investigations of polymorphism in phenalkylammonium salts and complexes of the general formula $C_6H_5C_nH_{2n}NH_3X$ (where $n = 1-10$ and X is Cl , Br , NO_3 , $CdCl_4$, $CuCl_4$, $CoCl_4$ and $ZnCl_4$) have been reported and reviewed [2, 3]. In general, most of these compounds were observed to undergo solid–solid phase transitions and the thermodynamics of the phase transitions were strongly influenced by the phenyl group. In these studies it was noted

* Corresponding author.

¹ Current address: Glaxo Research Institute, 5 Moore Dr., Research Triangle Park, NC 27709, USA.

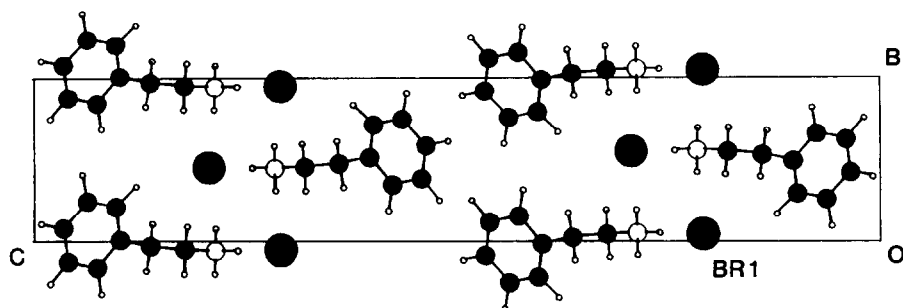


Fig. 1. A view of the unit cell of PhC2Br down the *a* axis. The large filled circles represent the bromide ions, the smaller open circle represents the nitrogen atom and the small closed circles represent the carbon atoms.

that DSC thermal curves obtained with phenethylammonium bromide $C_6H_5CH_2CH_2NH_3Br$ (PhC2Br) were influenced by particle size [2].

The crystal structure of PhC2Br is known. The unit cell is orthorhombic ($a = 4.675 \text{ \AA}$; $b = 6.145 \text{ \AA}$; $c = 31.975 \text{ \AA}$) and its crystal structure is described by the space group $P2_12_12_1$ with four formula units in the unit cell (Fig. 1) [4, 5]. The structure consists of infinite hydrogen-bonded chains where each hydrogen on the ammonium group is hydrogen-bonded to a different bromide ion to form a zig-zag chain. The chains are held together by van der Waals' forces.

Previous differential thermal analysis (DTA) investigations of the effect of particle size on the thermodynamics of solid–solid phase transitions in six different substances showed that the temperature of the solid–solid phase transition increased with a decrease in particle size [6]. It was suggested that if a phase transition proceeded by a cooperative mechanism it should be favored by large particles and require less thermal energy. These investigations also reported that the enthalpy of transition decreased with an increase in particle size, which was attributed to changes in the surface energies and surface area [6].

Investigations of hydrazinium sulfate $(NH_3NH_3)SO_4$ indicated that the two phase transformations had transition temperatures which were sensitive to particle size [7]. This compound had three crystal forms with a transition temperature of $\approx 220 \text{ K}$ for the Phase II to Phase III transformation and a transition temperature of $\approx 485 \text{ K}$ for the Phase II to Phase I transformation. The features of the Phase II to Phase III transformation could be summarized as follows.

- (1) The transition occurred over a very wide temperature range ($\approx 40 \text{ K}$).
- (2) The transition temperature shifted to successively lower temperatures (measured in the cooling direction) after repeated thermal cycling.
- (3) The fine structure in the DTA peaks disappeared gradually after repeated thermal cycling.

A 5 K temperature shift of the Phase II to Phase I transformation to

higher transition temperatures and the disappearance of the fine structure of the endotherm was also observed with thermal cycling.

Using sieved fractions, it was found that there was a decrease in transition temperature with a decrease in particle size (≈ 30 K) as measured by DTA in the cooling direction for the Phase II to Phase III transformation. The factors that could have given such a large supercooling were considered. It was concluded that not only interfacial energies were involved, but also some other kinetic factors. Such factors postulated were large molecular misfit across the boundary of the two phases and the facility with which the nucleus of the new phase is formed in the mother crystal.

In the case of the Phase II to Phase I transition, an adequate explanation could not be found for the observed increase in transition temperature with thermal cycling which was opposite to that of the Phase II to Phase III transition. It should be noted that the Phase II to Phase I transition was measured in the heating direction and the Phase II to Phase III transition was measured in the cooling direction.

Ammonium nitrate was also reported to produce complex DSC thermal curves with a considerable amount of fine structure [8]. No attempt was made to correlate transition temperature with particle size, but these investigators did find that different crystallites gave different transition temperatures when observed by DSC and hot-stage microscopy.

The purpose of this study was to investigate and document the thermodynamic properties of large single crystals and polycrystalline samples of phenethylammonium bromide using DSC.

EXPERIMENTAL

Phenethylamine $C_6H_5CH_2CH_2NH_2$ (Aldrich Chemical Company; Gold Label 99+ % pure) was used without further purification. PhC2Br was prepared by the neutralization of a diethylether + ethanol solution of phenethylamine with aqueous HBr. PhC2Br precipitated out upon addition of the HBr. It was suction filtered and washed several times with diethylether. PhC2Br was recrystallized twice from ethanol + diethylether and then dried under vacuum over P_2O_5 .

Large single crystals were grown by vapor exchange dilution. In dilution crystallization, a substance is added to reduce the solubility of the solute in the solvent. Figure 2 shows the apparatus used to grow the crystals. An open inner vial sits inside a larger screw cap vial. The inner vial contains the compound dissolved in methanol which is placed in a screw cap jar containing diethylether. Two criteria for solvent selection are (1) the compound must be soluble in one solvent but insoluble in the other solvent and (2) the two solvents must be miscible. When the apparatus is assembled, the diethylether evaporates and condenses into the methanol solution and the methanol evaporates and condenses into the diethylether.

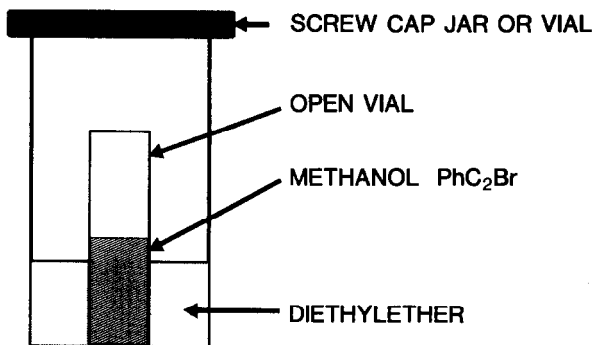


Fig. 2. The vapor exchange dilution crystallization system. An open inner vial contains PhC₂Br dissolved in methanol. The inner vial is placed in a large screw cap jar containing diethylether. The vapor exchange causes slow precipitation of the compound.

The final result is dilution of the methanol solution because the diethylether is more volatile. The rate of exchange can be varied by changing the temperature, selecting solvents of different boiling points and changing the size of the opening of the inner vial. In this case, needles of the PhC₂Br crystallized out. They were filtered and dried under vacuum over P₂O₅. Both large single crystals (10 mm × 1 mm × 1 mm) and polycrystalline samples were grown by this method. To obtain polycrystalline samples, the solution was rapidly stirred while the exchange was occurring.

X-ray powder diffraction patterns were obtained using a Philips PW1840 X-ray diffractometer system interfaced to an IBM PS2. Collection parameters for the X-ray diffractometer were as follows: scanning speed, 0.05 2θ min⁻¹; time constant, 1.0; slit width, 0.2; range, 0–35° 2θ; power, 40 kV, 30 mA. Samples were triturated using a mortar and pestle and the powder pattern was recorded. To obtain a powder pattern of the high temperature phase, the same sample was heated to ≈120°C for 60 min, quickly placed in the diffractometer and the powder pattern recorded.

Compressed KBr pellets of PhC₂Br were prepared and the IR spectra were obtained using a NICOLET FTS-7 Fourier transform IR (FT-IR) spectrometer recorded from 4000 to 400 cm⁻¹ with a 2 cm⁻¹ resolution. The spectrum was obtained at room temperature and then the same pellet was heated to 120°C for 10 min and the spectrum was obtained again. A spectrum identical to the original was obtained after leaving the sample at -30°C for 1 day.

Prior to DSC experiments, large single crystals were examined with a polarizing transmitted-light microscope to assess crystallinity and to look for other possible gross defects in the morphology. The polycrystalline samples were sieved through standard ASTM sieves and mesh fractions were collected.

DSC experiments were performed on a Perkin-Elmer DSC 4 with a System 4 controller interfaced to a Perkin-Elmer 3600 data station. Samples

(0.5–10 mg) were either sealed in volatile aluminum pans or placed in open aluminum pans. Typically, sample sizes of 1–2 mg were used to minimize the trade-off between the competing factors of sensitivity and thermal mass. Temperature and enthalpy calibrations were performed with an indium metal standard. Various scanning rates were used, ranging from 0.5 to $5^{\circ}\text{C min}^{-1}$; typically scan rates of $1^{\circ}\text{C min}^{-1}$ were used.

Hot-stage microscopy experiments were performed using a Carl Zeiss Universal R transmitted-light microscope fitted with a Mettler FP 82 hot stage. Temperature control was maintained using a Mettler FP 80 control unit.

PhC2Br was exposed to 90% relative humidity and the weight loss was measured as a function of temperature using a Perkin-Elmer thermogravimetric analyzer (TGS-2). From these experiments it was demonstrated that the compound was not hygroscopic, nor did it exist as a solvate. As a result, changes in the crystal structure could not be attributed to the presence of hydrates or solvates.

RESULTS AND DISCUSSION

Powder X-ray diffraction

Significant differences in the X-ray diffraction powder patterns of two apparent crystal forms is the definitive method of determining polymorphism. The X-ray diffraction powder pattern of PhC2Br at room temperature (RT) (Fig. 3) was indexed and found to be consistent with those calculated

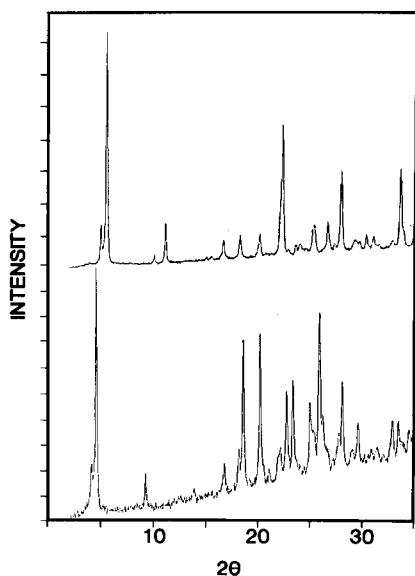


Fig. 3. X-ray diffraction powder patterns of PhC2Br. The upper powder pattern is a virgin sample at room temperature and the lower powder pattern is the same sample after heating to 120°C .

from reported single crystal diffraction data, indicating that sample preparation did not cause a phase change. The powder pattern obtained upon heating the sample to 120°C (Fig. 3) was different. The X-ray powder patterns were recorded with this high temperature (HT) phase and changes monitored as a function of time when this HT form was stored at ambient RT conditions. The HT phase gradually reverted to the RT phase. After 15 days at RT, there was evidence of the HT form in the powder pattern. To estimate the amount of the HT form present, a ratio of the intensity of the peak at $2\theta = 4.8$ obtained initially and after 15 days was determined. There appeared to be about 10% of the HT form remaining. When the sample was cooled to -30°C overnight, the RT form was regenerated. Apparently the recrystallization was slow at RT although the transition temperature is greater than 30°C above RT.

IR Spectroscopy

There is also spectroscopic evidence of polymorphism. Figure 4 shows the IR spectrum of the phenethylammonium bromide + KBr pellet at RT and the IR spectrum obtained when the sample was heated to 120°C. The spectrum of the HT form gradually returned to the spectrum of the RT form upon storing at room temperature. Like the X-ray powder patterns, features of the HT form can still be seen after 24 h at RT. After cooling the sample at -30°C overnight, the original RT spectrum was obtained.

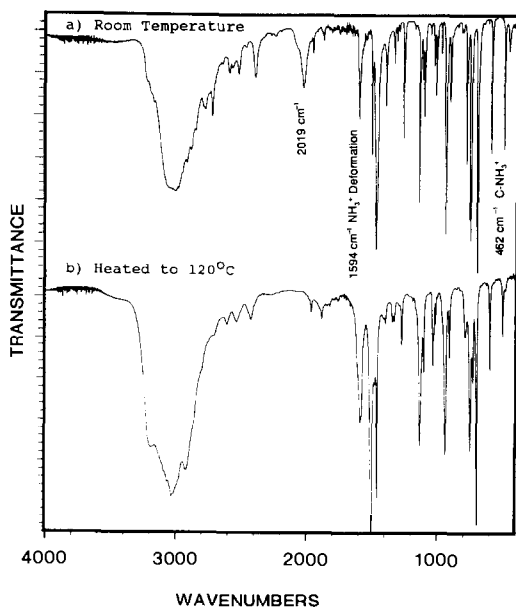


Fig. 4. Infrared spectra of PhC₂Br. The upper IR spectrum is a virgin sample at room temperature and the lower IR spectrum is the same sample after heating to 120°C for 30 min.

Upon conversion of the RT form to the HT form, a number of changes occurred in the IR spectrum. There were changes in the band splitting and in the shifting and disappearance of bands when the HT form was obtained. The most obvious change was the disappearance of the absorption at 2019 cm^{-1} when the sample was in the HT phase. In the $2100\text{--}1800\text{ cm}^{-1}$ region of the IR spectrum, combination bands of moderate intensity have been reported characteristic of the C-NH_3^+ grouping. These bands were assigned to a combination band of the C-NH_3^+ torsional oscillation (about 480 cm^{-1}) and the antisymmetric NH_3^+ deformation (about 1580 cm^{-1}) [9, 10]. Both of these modes are sensitive to hydrogen-bond strength. The combination modes are very sensitive because both the torsional and deformation frequencies will increase with the hydrogen-bond strength [9, 10]. In the case of PhC2Br, the absorption at 2019 cm^{-1} is probably a combination band of the absorption at 1594 and 462 cm^{-1} . The disappearance of the band at 2019 cm^{-1} and of the band at 462 cm^{-1} in the spectrum of the HT form supports this assignment (see Fig. 4).

Anilinium bromide $\text{C}_6\text{H}_5\text{NH}_3\text{Br}$ is reported to undergo a thermotropic solid–solid phase transition [11, 12] and the two crystal forms have been investigated by IR spectroscopy [13]. The low temperature form had an absorption at 2040 cm^{-1} which was not present in the HT form. This change in the IR spectrum was attributed to the NH_3^+ group going from a less than three-fold symmetry in the low temperature form to a HT form with three-fold symmetry [13].

These results suggest that the disappearance of the absorption at 2019 cm^{-1} in the HT form of PhC2Br may be due to a phase change to a structure of higher symmetry around the NH_3^+ group. The appearance of an intense shoulder at 3185 cm^{-1} in the HT phase further supports the hypothesis that the transition is partly due to a change in the NH_3^+ group dynamics.

DSC

When PhC2Br was recrystallized, the DSC thermal curve obtained indicated a broad transition with a considerable amount of fine structure (Fig. 5). When the sample was thermally cycled several times, the fine structure disappeared. The onset temperature T_o increased from about 70°C obtained for the original sample to 80°C for the thermally cycled sample (scanning rate, 5°C min^{-1} ; sample mass, 8.26 mg). The width at half height decreased from 10°C for the original sample to about 5°C for the cycled sample. Observing the phase transition microscopy under conditions similar to the DSC experiments, crystals shattered over a wide temperature as they transformed to the HT form producing smaller crystals. This physical phenomenon probably accounted for the observed fine structure and the

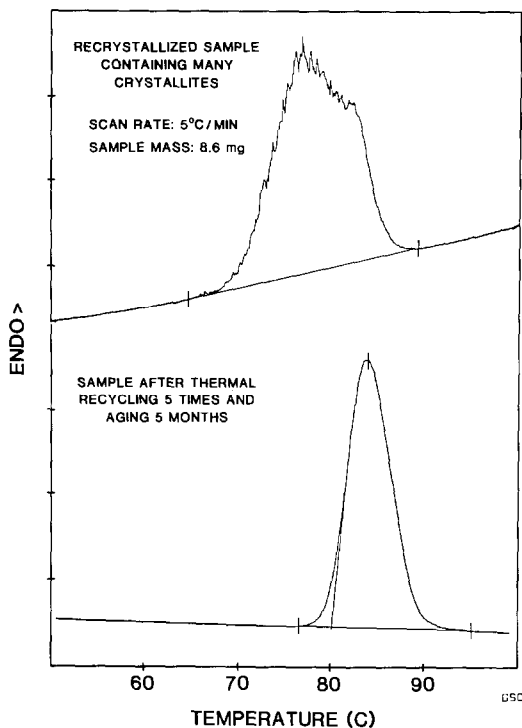


Fig. 5. DSC thermal curves of PhC₂Br. The upper DSC thermal curve is a freshly recrystallized sample and the lower thermal curve is the same sample after being thermally cycled five times and then left at room temperature for 5 months (scanning rate, 5°C min⁻¹; sample mass, 8.26 mg).

gradual change in the general characteristics of the DSC thermal curves upon thermal cycling. These general features of fine structure in the thermal curve, reduction in fine structure with thermal cycling, shattering of the crystal as it transformed into the other phase and changes in the onset temperature with thermal cycling were also reported in studies of hydrazinium sulfate [7].

The effect of DSC parameters (sample size and scan rate) on the onset temperature T_o of the solid–solid phase transition of a 325 mesh sieve fraction (45 μ m) was investigated. Scanning rates of 1 and 5°C min⁻¹ and sample sizes from 0.5 to 6 mg were used (Fig. 6). The value of T_o was observed to increase with an increase in scanning rate and sample size. The effect of sample size on T_o was similar at scanning rates of 1 and 5°C min⁻¹. With comparable sample sizes, the value of T_o obtained at 5°C min⁻¹ was about 4°C higher than that obtained at 1°C min⁻¹. Under the same conditions of scan rate and sample mass, the observed variation in the transition temperature was typically less than 1°C. Sources of error in the determination of T_o were partly due to the broadness and the fine structure of the endotherm produced by polycrystalline samples. It should be noted

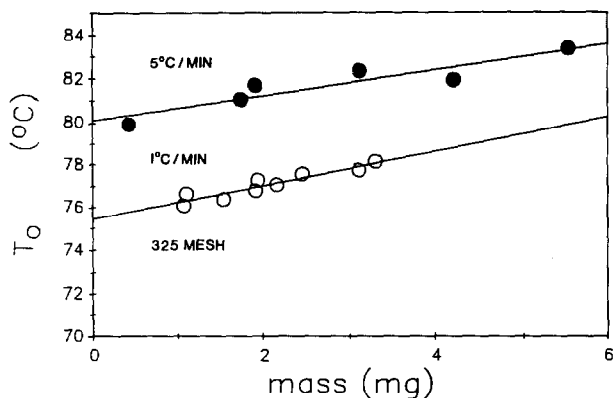


Fig. 6. A plot of onset temperature T_o vs. mass of 325 Mesh PhC2Br. The filled circles are the results at 5°C min^{-1} and the open circles are the results at 1°C min^{-1} .

that at a scanning rate of 1°C min^{-1} , T_o varied by about $\pm 1^\circ\text{C}$ for sample sizes of 1–4 mg.

To investigate the effect of particle size on the DSC thermal curves, recrystallized samples were classified with wire mesh sieves. Figure 7 shows

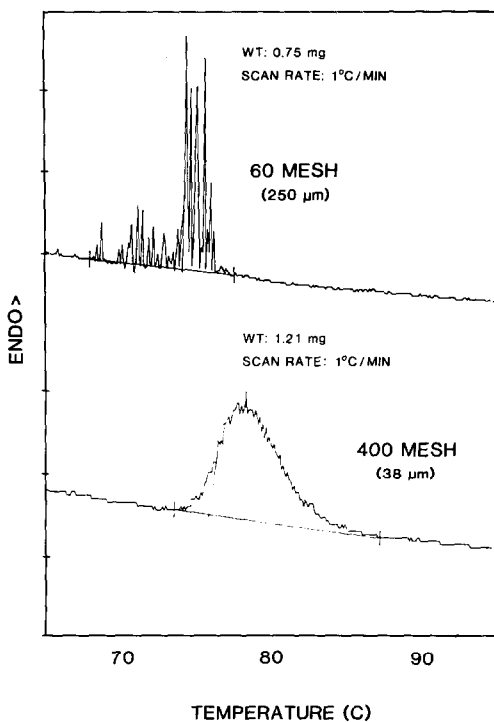


Fig. 7. DSC thermal curves of sieved fractions of PhC2Br. The upper thermal curve is the 60 Mesh ($250\ \mu\text{m}$) fraction and the lower thermal curve is the 400 Mesh ($38\ \mu\text{m}$) fraction (scanning rate, 1°C min^{-1}).

representative DSC thermal curves obtained with 1 mg samples scanned at $1^{\circ}\text{C min}^{-1}$ for the 60 mesh fraction ($250\ \mu\text{m}$) and the 400 mesh fraction ($38\ \mu\text{m}$). The 60 mesh sample, having larger particles, produced a thermal curve with many sharp peaks over a 10°C temperature range, suggesting that each of the individual crystallites underwent a transition at its own temperature. The 400 mesh sample, having smaller particles, produced a thermal curve with very little fine structure. This suggests that the thermal properties in these samples were more uniform. Each crystallite makes a small contribution to the composite peak. In general, the smaller particles have on average a higher transition temperature than the larger crystals. This supports results obtained after thermal cycling through the transition, the shattering of the crystals having reduced the particle size. This reduced the fine structure and increased the transition temperature. Similar features also were reported for hydrazinium sulfate [7].

DSC thermal curves of large crystals were obtained. Figure 8 shows the DSC thermal curve obtained for a single crystal of PhC2Br. The two most notable features are (1) that the phase transition is extremely sharp, the

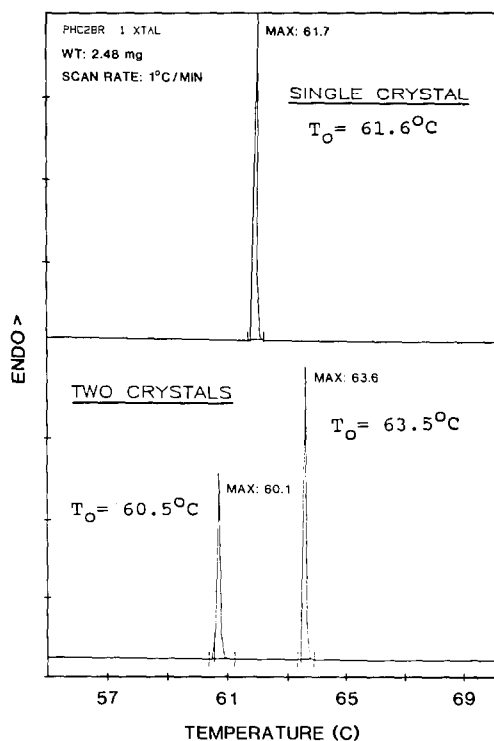


Fig. 8. DSC thermal curves of large crystals of PhC2Br. The upper thermal curve was obtained with one crystal: $T_o = 61.6^{\circ}\text{C}$; $T_{max} = 61.7^{\circ}\text{C}$. The lower thermal curve was obtained with two crystals in the same DSC experiment: $T_o = 60.5^{\circ}\text{C}$ and 63.5°C (scanning rate $1^{\circ}\text{C min}^{-1}$).

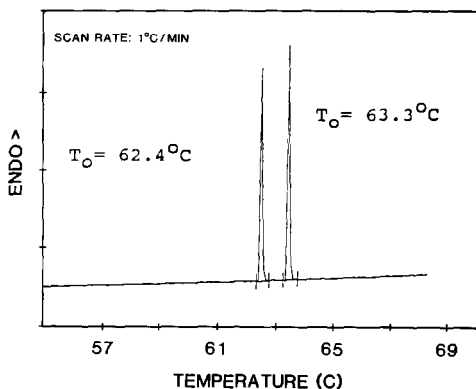


Fig. 9. DSC thermal curve of a large crystal of PhC₂Br cleaved into two crystals (scanning rate, 1°C min⁻¹).

onset temperature and the maximum temperature differing by about 0.1°C (the resolution of the instrument) and (2) that the transition temperature was 61.6°C for this particular sample, more than 10°C below T_o obtained for the polycrystalline sample.

Figure 8 also shows the DSC thermal curve for two crystals. Two peaks were obtained that were well-separated, with onset temperatures of 60.5°C and 63.5°C, a 3°C temperature difference. This was repeated for three crystals and four crystals, giving the same number of well-resolved peaks as crystals present. To reduce the differences that may be present between a random selection of crystals, a single crystal was cleaved. When scanned, two very sharp peaks were obtained that differed by $\approx 1^\circ\text{C}$ (Fig. 9). Similar results were obtained for cleaved crystals packed in aluminum powder (to improve thermal contact). As with any non-isothermal experiment, there are thermal gradients and non-equilibrium conditions which could account for some of the differences observed for T_o with different crystals, but these expected differences could not explain nor account for the observed differences.

These observations were confirmed by hot-stage microscopy experiments. In one experiment, two crystals were placed on the hot stage and the temperature was increased slowly. After one of the crystals shattered (63.1°C) the temperature was held constant. After 4 h at isothermal conditions the second crystal did not transform. The temperature was increased by 2°C and allowed to equilibrate for 6 h. The second crystal did not shatter. The second crystal did not shatter until the temperature was raised by about 4°C (66.9°C). Other hot-stage microscopy experiments indicated that the transition temperature was not a function of the orientation or position of the sample on the hot stage, but the transition temperature was highly variable, as was found with the DSC experiments.

The transition temperature was plotted against crystal mass to determine

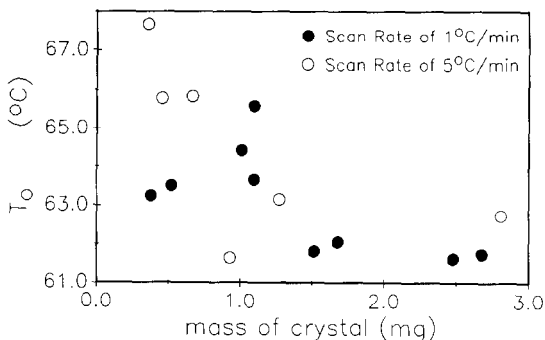


Fig. 10. A plot of onset temperature obtained from DSC experiments versus mass of a single crystal of PhC2Br. Open circles represent results obtained from scanning rates of $5^{\circ}\text{C min}^{-1}$ and filled circles represent results obtained from scanning rates of $1^{\circ}\text{C min}^{-1}$.

whether a correlation between mass of the single crystal and the transition temperature existed. Figure 10 is a plot of the onset temperature for the phase transition versus crystal mass for PhC2Br. The range of the transition temperatures observed was from $\approx 61^{\circ}\text{C}$ to 66°C , using scanning rates of $1^{\circ}\text{C min}^{-1}$; faster scanning rates ($5^{\circ}\text{C min}^{-1}$) did not improve the correlation or decrease the variability. The phase transition is very sharp for single crystals so the variation cannot be attributed to misinterpretation of the onset temperature. There does not appear to be a good correlation between sample mass and transition temperature. If thermal conductivity, thermal mass and thermal resistance were major factors, then one would have expected the larger crystals to have higher transition temperatures than the polycrystalline samples and the phase transition not to have been as sharp as observed. Because crystals are not free of defects and impurities, one would expect that the sharp phase transition would be very susceptible to the presence of these defects. This may be a contributing factor to the observed T_o variability.

Investigations of ammonium nitrate indicated that different crystals were undergoing the same phase transition at different temperatures [8]. In extreme cases, different crystals within the same sample had transition temperatures differing by about 10°C for the same phase transition. It was reported that the rate of movement of phase boundaries varied from crystallite to crystallite. Some movements were very slow (taking days to cross the field of view of the microscope). In other cases, the same phase transition could be completed in less than a second. These investigators believed that crystal defects (both lattice and impurity) were of key importance in determining T_o for the phase transitions in ammonium nitrate. This crystal-dependent behavior was attributed to the variety and frequency at which crystal defects occur.

The thermodynamics of the phase transition for single crystals ($\approx 1\text{ mm} \times 1\text{ mm} \times 3\text{ mm}$) and polycrystalline crystals (400 mesh; $\approx 38\ \mu\text{m}$)

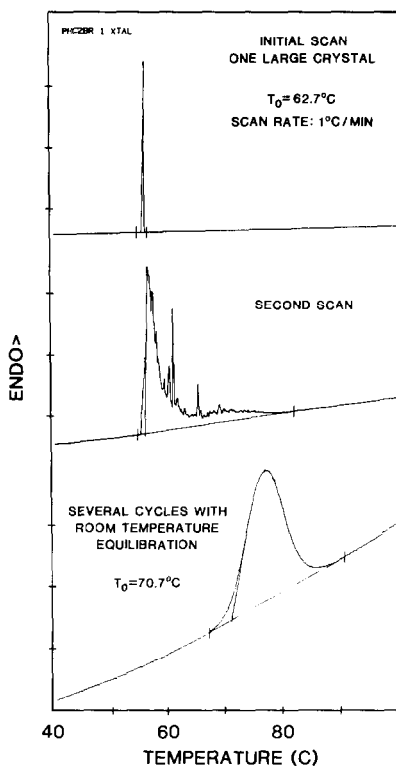


Fig. 11. DSC thermal curves showing the effect of thermal history: the upper thermal curve is a large crystal, $T_0 = 62.7^\circ\text{C}$; the middle thermal curve was obtained on the second scan; the bottom thermal curve was obtained after cycling from 25 to 100°C several times and storing at room temperature for five months.

of PhC₂Br were compared. There was significant variation in the observed T_0 and enthalpy of transition for the large crystals but the average transition temperature for the single crystals was 63°C (336 K) and the average enthalpy of the transition was 7136 J mol^{-1} . This corresponds to an entropy change of $2.55 R$ (assuming it is entirely first order). The average T_0 for the 400 mesh material was 76°C (349 K) with an average enthalpy of transition of 6620 J mol^{-1} , which corresponds to an entropy change of $2.28 R$. The same general results were obtained when a single crystal was thermally cycled (Fig. 11). A low temperature ($T_0 = 63^\circ\text{C}$) and high enthalpy of transition was observed initially. After thermally cycling, T_0 increased (by $\approx 10^\circ\text{C}$) and the enthalpy of the transition decreased (by $\approx 500\text{ J mol}^{-1}$). These results are contrary to the previously reported effects of particle size on the thermodynamics of solid–solid phase transitions. In this earlier study the enthalpy of transition was reported to increase with decreasing particle size [6].

It is difficult to explain why this opposite trend was observed. However, the current observations reported for PhC₂Br could be rationalized using

thermodynamic arguments. The entropy change is a measure of the change in order. A larger crystal should be more ordered because there should be fewer defects. As the particle size is decreased, there should be more defects and less order. This may explain the higher enthalpy and entropy of transition for large single crystals which decrease with particle size.

An approximate value of the entropy of transition ΔS_{TR} is given by eqn. (1).

$$\Delta S_{\text{TR}} = R \ln (N_2/N_1) \quad (1)$$

where R is the gas constant and N_2 and N_1 are the numbers of equivalent conformations accessible in the HT and low temperature phases, respectively. To approximate the increase in the number of conformations in the HT phase, one obtains a value for N_2/N_1 of 12.8 for the single crystal and 9.8 for the 400 mesh material. This suggests that the reduction in particle volume ($\approx 10^5$), or the corresponding increase in surface area, increases the disorder in the RT form and reduces the entropy of transition.

The increase in solid–solid phase transition temperature with a decrease in particle size is an interesting phenomenon which has been reported for other materials [6, 7]. A reduction in particle size increases the number of surface molecules and surface molecules have different physical properties from the molecules in the bulk. If crystals behave like liquid droplets, when there is a particle size reduction the crystal surface area has increased and the internal pressure of the bulk material has increased [14]. As with many phase transitions, the transition temperature increases with an increase in pressure. Therefore, the increase in transition temperature with particle size reduction may be related to an increase in internal pressure. In the case of liquid droplets, the pressure difference between the surface molecules and the molecules in the bulk can be calculated. This difference becomes substantial when the radius of curvature is small [14].

For large crystals there is a significant variation in transition temperature and enthalpy change, but, on average, the larger crystals have a lower transition temperature and higher enthalpy of transition than the smaller crystals. The probable cause of the observed variation in the larger and smaller crystals is kinetic and thermodynamic factors which are a function of the concentration of crystal defects, thermoconductivity, surface energy and surface tension.

With particle size reduction, there is, in general, an increase in transition temperature, a decrease in the entropy of transition and a decrease in fine structure of the thermal curve. Particle size reduction can be accomplished mechanically or by thermal cycling (because the crystals shatter when they undergo the phase transformation). Similar results have been reported for hydrazinium sulfate. As the particle size is reduced, it requires more thermal energy to induce the phase change. If the phase change is a cooperative phenomenon and/or is related to the change in internal

pressure of the crystal then this would be the predicted trend that one would expect.

Although the observed thermal behavior of the solid–solid phase transition of PhC₂Br is rare, it is not unique. It is interesting to note that, to date, ammonium salts are the only materials for which this phenomenon has been observed. However, phenethylammonium chloride, which is isostructural but undergoes two solid–solid phase transitions, did not show this behavior [2]. Several factors probably involved in the thermal behavior of these salts may include the different types of change occurring with the molecular interactions of the different crystal forms.

ACKNOWLEDGMENTS

M.J.M.V.O. thanks MFCI and the Natural Sciences and Engineering Research Council of Canada for grants and support.

REFERENCES

- 1 N.G. Parsonage and L.A.K. Staveley, *Disorder in Crystals*, Clarendon, Oxford, 1978.
- 2 M.J.M. Van Oort and M.A. White, *Thermochim. Acta*, 139 (1989) 205.
- 3 M.J.M. Van Oort and M.A. White, *J. Solid State Chem.*, 75 (1988) 113.
- 4 G. Tsoucaris, *Acta Crystallogr.*, 14 (1961) 909.
- 5 T.S. Cameron, O. Knop and S. Roe, unpublished work, 1986.
- 6 M. Natarajan, A.R. Das and C.N.R. Rao, *Trans. Faraday Soc.*, 65 (1969) 3081.
- 7 T. Okamoto, N. Nalamura, and H. Chilhara, *Bull. Chem. Soc. Jpn.*, 52 (1979) 1619.
- 8 J.S. Ingman, G.J. Kearly and S.F.A. Kettle, *J. Chem. Soc. Faraday Trans. 1*, 78 (1978) 1817.
- 9 N.B. Colthup, L.H. Daly and S.E. Wiberley, *Introduction to Infrared and Raman Spectroscopy*, Academic Press, New York 1964, p. 281.
- 10 I.A. Oxtton and O. Knop, *J. Mol. Struct.*, 43 (1978) 17.
- 11 G. Fecher, A. Weiss, W. Joswig and H.Z. Fuess, *Z. Naturforsch. Teil A*, 36 (1981) 956.
- 12 G. Fecher, A. Weiss, and G.Z. Heger, *Z. Naturforsch. Teil A*, 36 (1981) 967.
- 13 A. Cabana and C. Sandorfy, *Can. J. Chem.*, 40 (1962) 622.
- 14 I.N. Levine, *Physical Chemistry*, McGraw-Hill, New York, 1978.